

# Frequency-dependent radiation patterns emitted by THz plasmons on finite length cylindrical metal wires

Jason A. Deibel, Nicholas Berndsen, Kanglin Wang, Daniel M. Mittleman

Department of Electrical and Computer Engineering, MS 366, Rice University, Houston, Texas 77251-1892  
[daniel@rice.edu](mailto:daniel@rice.edu)

Nick C. J. van der Valk and Paul C. M. Planken

University of Technology Delft, Faculty of Applied Sciences, Lorentzweg 1, 2628 CJ Delft, the Netherlands  
[P.C.M.Planken@tudelft.nl](mailto:P.C.M.Planken@tudelft.nl)

**Abstract:** We report on the emission patterns from THz plasmons propagating towards the end of cylindrical metal waveguides. Such waveguides exhibit low loss and dispersion, but little is known about the dynamics of the terahertz radiation at the end of the waveguide, specifically in the near- and intermediate-field. Our experimental results and numerical simulations show that the near- and intermediate-field terahertz spectra, measured at the end of the waveguide, vary with the position relative to the waveguide. This is explained by the frequency-dependent diffraction occurring at the end of the cylindrical waveguide. Our results show that near-field changes in the frequency content of THz pulses for increasing wire-detector distances must be taken into account when studying surface waves on cylindrical waveguides.

©2006 Optical Society of America

**OCIS codes:** (240.6680) Optics at surfaces: Surface plasmons; (230.7370) Optical devices: Waveguides; (260.3090) Physical Optics: Infrared, far

---

## References and Links

1. K. Wang, A. Barkan, and D. M. Mittleman, "Propagation effects in apertureless near-field optical antennas," *Appl. Phys. Lett.* **84**, 305-307 (2004).
2. K. Wang and D. M. Mittleman, "Metal wires for THz wave guiding," *Nature (London)* **432**, 376-379 (2004).
3. T. Jeon, J. Zhang, and D. Grischkowsky, "THz Sommerfeld wave propagation on a single metal wire," *Appl. Phys. Lett.* **86**, 071106/1-3 (2005).
4. M. Wächter, M. Nagel, and H. Kurz, "Frequency-dependent characterization of THz Sommerfeld wave propagation on single wires," *Opt. Express* **13**, 10815-10822 (2005).
5. K. Wang and D. M. Mittleman, "Dispersion of surface plasmon polaritons on metal wires in the terahertz frequency range," *Phys. Rev. Lett.* **96**, 157401/1-4 (2006).
6. N. C. J. van der Valk and P. C. M. Planken, "Effect of a dielectric coating on terahertz surface plasmon polaritons on metal wires," *Appl. Phys. Lett.* **87**, 071106/1-3 (2005).
7. N. C. J. van der Valk, "Towards terahertz microscopy," thesis, [http://www.library.tudelft.nl/dissertations/dd\\_list\\_paged/dd\\_metadata/index.htm?docname=363824](http://www.library.tudelft.nl/dissertations/dd_list_paged/dd_metadata/index.htm?docname=363824).
8. M. Walther, M. R. Freeman, and F. A. Hegmann, "Metal wire terahertz time-domain spectroscopy," *Appl. Phys. Lett.* **87**, 261107/1-3 (2005).
9. M. Walther, G. S. Chambers, Z. Liu, M. R. Freeman, and F. A. Hegmann, "Emission and detection of terahertz pulses from a metal-tip antenna," *J. Opt. Soc. Am. B* **22**, 2357-2365 (2005).
10. M. I. Stockman, "Nanofocusing of optical energy in tapered plasmonic waveguides," *Phys. Rev. Lett.* **93**, 137404/1-4 (2004).
11. F. Hao and P. Nordlander, "Plasmonic coupling between a metallic nanosphere and a thin metallic wire," *Appl. Phys. Lett.* **89**, 103101 (2006).
12. G. Zhao, R. N. Schouten, N. C. J. van der Valk, W. Th. Wenckebach, and P. C. M. Planken, "Design and performance of a THz emission and detection setup based on a semi-insulating GaAs emitter," *Rev. Sci. Instrum.* **73**, 1715-1719 (2002).
13. J. A. Deibel, K. Wang, M. D. Escarra, and D. M. Mittleman, "Enhanced coupling of terahertz radiation to cylindrical wire waveguides," *Opt. Express* **14**, 279-290 (2006).

14. K. Wang, D. M. Mittleman, N. C. J. van der Valk, and P. C. M. Planken, "Antenna effects in terahertz apertureless near-field optical microscopy," *Appl. Phys. Lett.* **85**, 2715 (2004).
  15. G. Goubau, "Surface waves and their application to transmission lines," *J. Appl. Phys.* **21**, 1119-1128 (1950).
  16. J. Jin, *The Finite Element Method in Electromagnetics*, (John Wiley & Sons, Inc., New York 2002).
- 

## 1. Introduction

Recently, several reports have shown that cylindrical metal wires can act as waveguides for terahertz (THz) pulses [1, 2, 3]. The THz pulses propagate on these wires as surface plasmon polaritons having a radial polarization and are often referred to as Sommerfeld waves [3, 4]. It has been shown that these pulses can travel relatively long distances of up to a few meters on these wires, since they experience little attenuation [2, 3]. The dispersion experienced by the surface waves, however, is dependent on the diameter of the wire. For thick wires, with a diameter of 1 mm and larger, the dispersion is small. Recently, however, it was found that the dispersion increases strongly for thinner wires [5]. One of the remarkable properties of THz surface waves on metals is that the penetration depth of the THz electric field inside the metal is in the tens of nm's range, whereas the penetration depth in the air surrounding the wire is on the order of several mm's to cm's, depending on frequency. Thus, changes in the immediate environment of the wire, such as a surface coating, can affect the propagation of the pulses, giving rise to dispersion [6, 7] and absorption [8].

In most of the cases cited above, the THz surface waves are measured by allowing them to propagate towards the end of the wire followed by detection using either photoconductive dipole antennas, or electro-optic sampling. Walther et al. studied the far-field angular emission patterns from long metal tips and showed that they function like THz traveling wave antennas [9]. So far, however, little attention has been paid to the near-field and intermediate-field spectral and spatial properties of the wave emitted at the end of the wire. To our knowledge, analytical expressions describing the near-field of the end of a cylindrical wire do not exist, since the finite thickness of the wire, which is on the order of the wavelength, must be taken into account. This lack of both experimental and theoretical information is unfortunate, as the transition from the near-field to the far-field is quite relevant to many of the recent measurements. We also note that the propagation of cylindrically symmetric surface plasmons on metallic nanowires, and in particular their behavior near the ends of these nanostructures, has been a subject of much recent interest in the nanophotonics literature [10,11] The details of the coupling of these surface modes to propagating modes, as characterized by the near-field to far-field transition, must be understood before a meaningful interpretation of the experimental results can be made.

Here we present measurements and numerical calculations on the spatial dependence of the near- and intermediate field spectra emitted by THz surface waves near the end of cylindrical wires. These measurements were performed in two different laboratories using different wire diameters and show similar results. We find that the spectral content of the THz pulses emitted from the end of the wire changes as a function of the distance between the detector and the wire. When the distance between the detector and the wire is increased in the direction of the long axis of the wire, the spectral maximum of the measured THz pulse shifts to higher frequencies. 3D numerical calculations show that this can be explained by the frequency dependent diffraction that occurs at the end of the wire when the THz surface wave radiates energy into free space. Our results clearly demonstrate that near-field changes in the frequency content of THz pulses for increasing wire-detector distances must be taken into account when studying surface waves on cylindrical waveguides.

## 2. Experimental setup

The experimental setups used for these measurements are indicated in Fig. 1. In one setup, THz pulses from a photoconductive switch [12] are focused onto a sharp copper tip held close to a stainless steel wire with a 1 mm diameter. The copper tip is used to scatter the THz pulse onto the stainless steel wire by creating THz polarization components that correspond to

modes of propagation of a surface wave on the cylindrical waveguide [2]. Of these modes, only a single, radially polarized mode survives after propagating along the length of the wire for several cm's. While it has been shown that this scattering technique is not the most efficient method of coupling terahertz radiation to a wire waveguide [13], it is a simple and effective method, and is adequate for these measurements. The surface wave propagates towards the end of the wire where it is partially scattered into free space. The end of the wire is held close to the surface of an electro-optic ZnTe crystal with a thickness of 1 mm. The crystal is mounted on a translation stage to vary the distance between the crystal and the waveguide. From the back, a synchronized probe pulse is focused, using a 10 cm focal length lens, onto the front surface of the crystal. The probe pulse is reflected from the front surface and sent to a standard differential detection setup. In the crystal, the THz electric field elliptically polarizes the probe pulse, where the amount of ellipticity is proportional to the electric field strength. The crystal has a (110) orientation ensuring that only THz electric field components in a plane perpendicular to the length of the waveguide, parallel to the crystal surface, are measured. The signal from the differential detector is digitized using a digital oscilloscope and by varying the time delay between the probe pulse and the THz pulse, the full time-dependent electric field of the THz pulse is obtained. In the electro-optic detection setup, whenever the position of the crystal is changed, small corrections in the beam path are necessary to keep the probe beam fixed on the differential detector.

In the second setup, the THz pulses are generated and detected using a fiber-coupled photo-conductive emitter and detector. The advantage of the fiber coupling is that it allows for greater flexibility than the electro-optic setup as no realignment is necessary when the distance between the waveguide and the detector is varied. As in the first setup, only the component of the electric field in a plane perpendicular to the length of the wire is measured. The spatial resolution of the setup is limited to a value of approximately 6 mm, corresponding to the aperture of the substrate lens. The advantage of the lens is that it collects and concentrates the field over a larger area, giving rise to stronger signals. As we will show below, the results obtained with this setup were similar to the results obtained with the setup shown in Fig. 1(a). A scattering mechanism, similar to that employed in the first experiment,

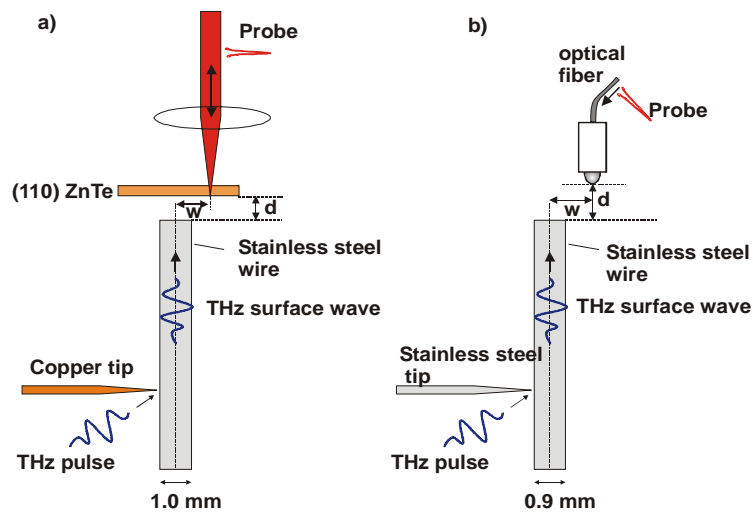


Fig.1. (a). Schematic diagram of the setup used to measure the emission from surface waves near the end of a 1 mm diameter stainless steel wire. The THz electric field is measured using electro-optic detection in a (110) oriented ZnTe crystal. (b) Schematic diagram used to measure the THz electric field present near the end of a 0.9 mm diameter stainless steel waveguide using fiber-coupled THz emitters and detectors. In both figures,  $w$  is the transverse separation between the center of the waveguide and the position where the field is measured.  $d$  is the longitudinal distance.

is used to couple the THz pulses onto a 0.9 mm diameter stainless steel wire. A second stainless steel coupling wire, of identical diameter, is placed approximately 500 microns from the waveguide wire, but in a direction normal to it. The THz pulses are focused onto the gap between the two wires and are scattered and a small amount of the terahertz radiation is coupled onto the mode of the waveguide. The THz electric field near the end of the waveguide is measured with a detector mounted on an XYZ -translation stage. The stainless steel wires used in the first experiment were cut using pliers, while the wires for the second experiment were cut by the vendor, providing reasonably smooth and flat ends in comparison to the wavelengths measured.

### 3. Results

In Fig. 2(a) we plot the amplitude spectra of the THz transients measured at the end of the 1 mm diameter stainless steel wire using the setup depicted in Fig. 1(a), for seven values of  $d$ , obtained at a transverse distance  $w = 1$  mm [see also Fig. 1(a)]. At  $d = 0$  mm, the figure shows a spectrum which peaks around 0.11 THz and tapers off to zero for frequencies approaching 1 THz. When the distance between the wire and the EO-crystal is increased from  $d=0$  mm to  $d=4.24$  mm, the peak amplitude of the spectral maximum decreases. More importantly, the relative contribution to the spectrum of frequency components between 0.11 and 0.4 THz increases, giving rise to a shift of the spectral maximum from 0.11 to 0.2 THz. We note that the measurements have to be taken at finite values of the transverse distance  $w$  between the center of the wire and the detector. This is because for radially polarized surface waves, the field beyond the end of the wire is zero on a line which coincides with the center of the wire [2].

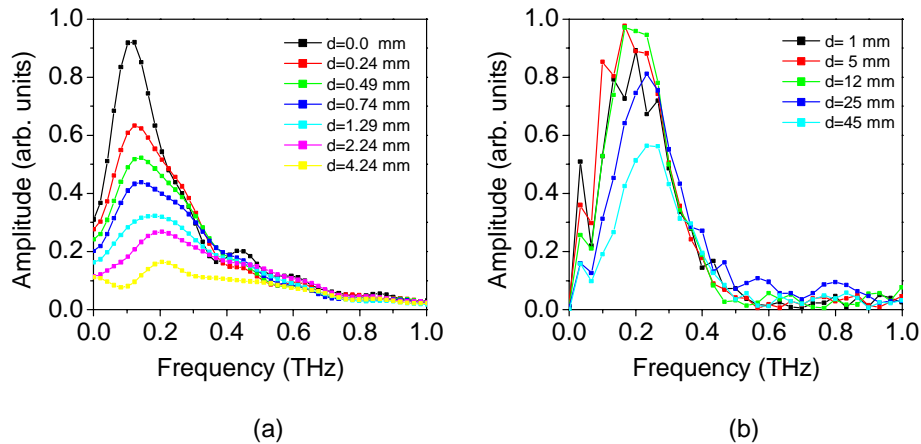


Fig. 2. (a). THz spectra measured near the end of the 1 mm diameter stainless steel wire at a transverse separation  $w=1$  mm, for seven values of the distance  $d$  between the detector and the end of the wire [see Fig. 1 (a)]. (b) THz spectra measured near the end of the 0.9 mm diameter stainless steel wire at a transverse separation of  $w = 2$  mm, for five values of the distance  $d$ . [see also Fig. 1 (b)]

In Fig. 2(b) we plot the amplitude spectra measured at the end of the 0.9 mm diameter wire using the setup depicted in Fig. 1(b), for five values of the distance  $d$ , obtained at a transverse distance  $w=2$  mm. Here, at the shortest distance  $d=1$  mm, the spectral maximum occurs at a somewhat higher frequency of around 0.2 THz. When the distance is increased to values larger than  $d=12$  mm, the spectral maximum shifts to a higher value of around 0.25. Similar results are obtained by selecting other transverse distances and analyzing the THz radiation as

a function of the distance away from the end of the wire. The values of  $d$  for which a reasonable signal can still be measured are considerably larger than those shown in Fig. 2(a). This is caused by the fact that the 6 mm diameter lens on the detector collects the radiation from a larger area and concentrates it to create a higher field-strength. In the electro-optic detection method, there is no lens to concentrate the radiation resulting in a higher spatial resolution but at the expense of a smaller signal. We would like to point out that in spite of the fact that these results were obtained in different laboratories using different laser systems the results shown in Fig. 2(b) are remarkably similar to the results shown in Fig. 2(a). The difference is that in Fig. 2(b) the shift in the spectral maximum towards higher frequencies is only visible for distances larger than 12 mm. As mentioned before, it is likely that the 6 mm diameter of the lens on the THz photoconducting emitter in this experiment reduces the spatial resolution, potentially masking small shifts in the spectral maximum for  $d < 12$  mm.

It is interesting to note that the bandwidth of the pulses measured after propagation off the end of the waveguide, is considerably smaller than the bandwidth of the incident pulses. The precise explanation for this is not known, but we would like to point out that metal wires are known to act as low-pass filters for incident THz pulses [14]. Since our experiments involve two wires, one to couple THz pulses to the waveguide, and the cylindrical wire itself, a smaller bandwidth is to be expected.

#### 4. Calculations and discussion

To understand the results shown in Fig. 2, we have performed 3D ( $x,y,z$ ) numerical simulations on a cylindrical wire. These simulations were designed and conducted using COMSOL Multiphysics, a commercially available finite element method modeling software. These calculations, based on the finite element method (FEM), simulate the propagation of a Sommerfeld wave [15] along a wire waveguide. A 0.9 mm diameter waveguide, 2.5 cm long, is placed inside of a cylindrical domain (3.75 cm in length, 6.5 mm in diameter) that bounds the volume of the simulation. The Sommerfeld wave is excited by assigning a time-varying electric field to one of the circular bases of the cylinder. This electric field excitation is based on an analytical solution describing the propagation of a Sommerfeld wave. At the opposite side of the cylinder, an additional domain, in the shape of a truncated cone, is added to allow for the spreading of the terahertz wave as it propagates off of the end of the waveguide. For a study of the propagation effects at just the end of the waveguide, the large simulation domain may at first seem unnecessarily large. However, a long extent of waveguide is required in order that the excited THz surface wave exhibits stable propagation. All external boundaries, with the exception of where the Sommerfeld wave is excited, are defined as “matched” boundaries which minimize the possibility of any EM waves back reflecting at the boundaries. The wire waveguide’s outer boundary is defined as a transition boundary condition using the surface impedance of the metal and the finite conductivity of the metal. There is a decent amount of variation for these dielectric parameters for differing types of metals and specifically for stainless steels. However, our simulations show that while these parameters will affect the loss and dispersion exhibited by the wire waveguide, varying their actual value does not affect the diffraction effect observed at the end of the wire. Prior to computation, the model is discretized into over 1.5 million mesh elements. The solution is obtained using an iterative solver that employs the Generalized Minimal Residual (GMRES) method with Symmetric Successive Overrelaxation (SSOR) matrix preconditioning. The solver is time-harmonic, so only one frequency is computed at a time. Using a workstation with dual 64-bit processors and 16 GB of RAM, a solution is typically obtained after 3 hours of computational time.

While it is true that taking advantage of radial symmetry would decrease the computation time and memory requirements of our simulations by reducing the model to a 2D problem, we chose to model in three dimensions to allow for easier post-processing and visualization of the results. Computer limitations also constrain the frequencies that can be simulated. At least three, but often more, mesh elements per wavelength are required in order for an electromagnetic wave to propagate in a FEM simulation [16]. For a simulation such as the one

described here where the wavelength can be less than a mm but the simulation domain is several cm long, this mesh density requirement results in an increasingly large number of mesh elements as the frequency increases. For this particular model, these consideration constrain our simulation results to frequencies under 150 GHz.

In Fig. 3, we show 2D images of the calculated spatial distribution of the THz intensity at and around a 0.9 mm stainless steel wire, for frequencies of 50, 75, 100, 125, and 150 GHz. The intensities are shown in a plane (x-z) which contains the long axis of the wire. Note that although the range of frequencies does not fully overlap the frequency range employed in the experimental results, the aim is to obtain a qualitative understanding of the observed changes in the measured spectra as a function of the distance from the end of the wire. The color scale in the graphs is saturated, in order to highlight the emission from the end of the wires. The higher intensity near the wire is indicated in white. The figures allow us to draw a number of conclusions. First, as expected, no light is visible on the wire axis beyond the end of the wire. This can be understood from the fact that the mode is radially polarized on the symmetric waveguide. Components of the electric field parallel to the flat end, resulting from diffraction from opposite sides of the waveguide, are always 180 degrees out of phase and thus cancel

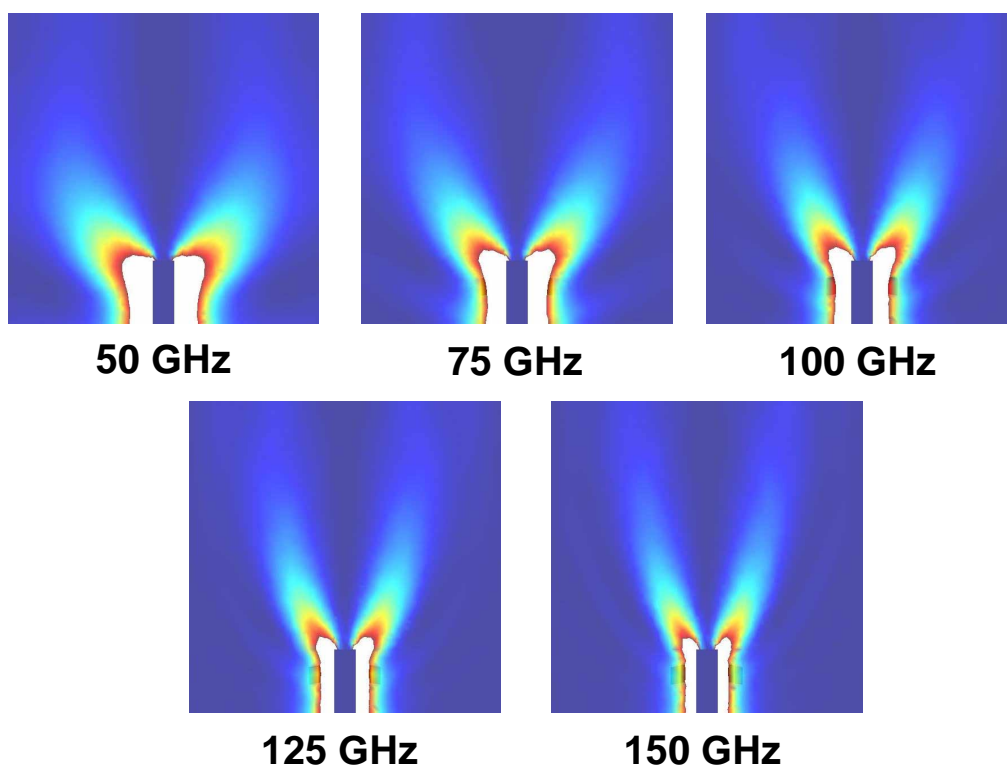


Fig. 3. Calculated THz intensity distribution in a plane containing the axis of a 0.9 mm thick wire, for five different frequencies. Red indicates a high intensity, blue indicates a low intensity. The color scale in these images has been saturated to enhance the visibility of the fields propagating away from the end of the wire. The higher intensities near the wire are therefore beyond the limits of this saturated color scale, and are depicted in white.

exactly in the middle. The intensity is also zero at the centre, exactly at the metal flat end, even though an electric-field component perpendicular to the metal is, in principle, allowed. Apparently, the radially polarized mode does not allow for such a component to be generated for this particular shape of the waveguide, which is consistent with the measurements. The figures also clearly show that at the end of the wire, the radiated field forms a conical

emission pattern propagating into free space. Both the cone opening angle and the width of the conical beam change as the frequency increases, with the width becoming narrower and the angle becoming smaller. These changes are caused by frequency-dependent diffraction, giving rise to a broader beam for lower frequencies. At the end of the wire, THz surface waves are scattered into propagating waves, which diffract off the edges of the cylinder surface with the diffraction being stronger for the low frequencies than for the high frequencies. It is also possible that there is an end-face reflection of the THz surface wave at the end of the wire due to the impedance mismatch there. As these simulations were performed in the frequency domain, it is difficult to observe such phenomenon. Future time-domain based simulations may reveal further insight into the end-face reflectivity and its relationship to the frequency-dependent diffraction at the end of the wire observed here.

We are now in a position to understand the measurements shown in Fig. 2. The measurements were performed along a line parallel to the wire but slightly displaced to the right. From the plots shown in Fig. 3, it can be deduced that along this line, while moving away from wire end, the intensity of the lower frequencies decreases faster than the intensity of the higher frequencies. Figure 2 demonstrates that this is precisely what is observed in the experiment. Our results prove that in the near- and intermediate field region around the wire end, the measured spectrum emitted by the surface waves is a function of position, and moreover that this functional dependence is rather complicated. This information is essential in studies of surface waves on cylindrical waveguides and must be considered when interpreting measured spectra.

## 5. Conclusion

We have performed measurements and calculations of the THz electric field propagating off the end of cylindrical metal wires which show that the near- and intermediate field, the spectra are a function of position with respect to the wire end. In general we find that the spectral maximum shifts to higher frequencies when moving away from the wire end along a line parallel to the wire. We attribute these changes to the frequency-dependent diffraction of THz pulses off the metal wire, which is stronger for low frequencies. Our results provide important information for researchers studying surface waves on cylindrical metal waveguides or on metal nanowires.

## Acknowledgments

The work at Delft University of Technology was performed as part of the "Stichting for Fundamenteel Onderzoek der Materie (FOM)", which is financially supported by the "Nederlandse organisatie voor Wetenschappelijk Onderzoek (NWO)."

The work conducted at Rice University was funded in part by the National Science Foundation, the R. A. Welch Foundation, and the Intelligence Community Postdoctoral Fellowship Program.